Elastic scattering of intermediate-energy electrons by Ar and Kr

S. K. Srivastava, H. Tanaka,* A. Chutjian, and S. Trajmar
Jet Propulsion Laboratory, California Institute of Technology, Pasadena, California 91103
(Received 3 June 1980)

Using the relative-flow technique elastic differential cross sections σ_θ (Ar or Kr) for Ar and Kr relative to σ_θ (He) have been measured at impact energies of 3, 5, 7.5, 10, 15, 20, 30, 50, 75, and 100 eV. The angular range covered is from 20° to 135°. These ratios have been multiplied by the recently measured values of σ_θ(He) to obtain σ_θ(Ar or Kr). The differential cross section curves for both Ar and Kr show deep minima. The positions of these minima have been obtained with an accuracy of ±2°. The cross sections in the angular regions lying between 0° and 20° and 135° and 180° could not be measured owing to instrumental limitations. In these regions estimates of the shapes of differential cross section (DCS) curves have been made by fitting the data obtained from 20° to 135° with a phase-shift analysis, while the normalization to the absolute scale was obtained by normalizing these fits to the relative flow measurements. From these estimates and the measured values of the differential cross section, integral and momentum-transfer cross sections have been obtained. The error limits for the differential, integral, and momentum-transfer cross sections have been estimated as 20, 30, and 30%, respectively.

I. INTRODUCTION

Electron-impact studies of rare-gas atoms have been of great interest since the 1930's. Recently, rare-gas–halide high-power lasers have sparked new interest in the electron collision cross sections for these atoms. From the point of view of either theoretical models or practical applications, absolute values for electron–rare-gas-atom cross sections as a function of electron-impact energy are needed. The electron-impact energy region between 1 and 100 eV (generally defined as the intermediate energy region) is of special interest because the values of collision cross sections are large and have maxima in this energy range. For Ar and Kr a uniform set of absolute cross sections covering this energy region is not available.

A survey of experimental and theoretical work prior to 1977 is given in a recent review paper by Bransden and McDowell.[1] The momentum-transfer cross sections have been measured by Frost and Phelps.[2] The elastic-scattering differential cross sections have been summarized for Ar and Kr by Jansen *et al.*[3] and Jansen and de Heer,[4] respectively. Since the review of Bransden and McDowell several experimental and theoretical papers have appeared and they are described below. de Heer *et al.*[5] suggested the values of total excitation, ionization, and scattering cross sections for both species utilizing all available data and a semiempirical approach. Williams[6] measured elastic-scattering angular distributions for Ar at 22 impact energies ranging from 0.58 to 20 eV and analyzed his data in terms of real s, p, d, and f phase shifts (Andrick[7] has also obtained angular distributions for Ar below 20 eV and has derived s-, p-, d-, and, f-wave phases from these data). Guskov[8] reported integral elastic cross sections for both Ar and Kr in the 0.025 to 1 eV impact energy range. Yau *et al.*[9] calculated elastic cross sections for both Ar and Kr using a polarized orbital method and adiabatic local exchange approximation. In addition, at and above 100 eV, Khare and Kumar[10] and Roy and Sil[11] carried out theoretical calculations. The measurements that have been reported in the past are either only at a few electron-impact energies or are relative in nature. This situation is especially true in the case of inelastic differential cross sections (DCS).

As a first step in a systematic study of the rare gases we have measured differential cross sections for the elastic scattering of electrons by Ar and Kr in the energy region between 3 and 100 eV. At each impact energy an angular range of 20° to 130° (or 135°) has been covered. The differential cross sections for exciting various bound states below the first ionization threshold have also been measured and are reported elsewhere.[12,13]

II. EXPERIMENTAL APPARATUS AND METHOD

A. Experimental apparatus

The experimental procedures and the details of the apparatus used in the present measurements have been described previously.[14,15] Briefly, the apparatus consists of an electron scattering spectrometer, gas flow system, and a multichannel analyzer for detecting and storing the scattered electron signal.

The scattering spectrometer contains an electron gun and hemispherical monochromator which produces a nearly monoenergetic electron beam of the desired energy, a detector with a hemispherical electron energy analyzer and a spiraltron for the detection of scattered electrons; and a capillary array through which Ar or Kr gas effuses to pro-

duce a well-defined beam of these atoms. The incident electron beam crosses the atomic beam at 90°. Owing to mechanical limitations the scattered electrons can be detected only in the angular region between −30° and 135° with respect to the direction of the incident electron beam. During the present measurements the overall resolution of the spectrometer was 60 meV although the spectrometer is capable of higher resolution.

The gas flow system used in the present measurements consisted of two gas lines which were connected to the capillary array through two precision gas flow valves, two flowmeters, and a precision pressure gauge. The details of this arrangement are given in Ref. 15 (Fig. 1). One of the gas lines was connected to the Ar or Kr gas cylinder and the other was connected to a He gas cylinder. Pure research grade gases were used. This gas flow system permitted the formation of a gas beam of He, Ar, or Kr by opening the appropriate precision flow valve. The scattered electrons were energy analyzed, detected, and stored in a multichannel analyzer utilizing pulse counting techniques.

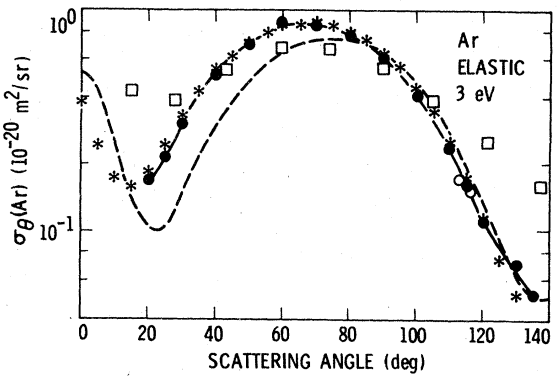

FIG. 1. Differential cross section for the elastic scattering of 3-eV electrons by Ar. *Andrick (Ref. 7), □ Ramsauer and Kollath (Ref. 17), --- Walker (exch +pol) (Ref. 18), • present, joined by a best visual fit solid line.

B. Cross-section calibration method

The details on the theoretical background of the method can be found in Ref. 15. The method employs a measurement of the ratio of the elastically scattered intensity of either Ar or Kr to that of He. At the same time the flow rates and pressures behind the capillary array are measured. First a beam of Ar (or Kr) is formed by flowing the appropriate gas through the capillary array. The elastically scattered electron intensity $[\dot{N}_e(\mathrm{Ar,Kr})]$ at angles varying from 20° to 135° is recorded. The Ar (or Kr) gas is then replaced by He and the scattered intensity $[\dot{N}_e(\mathrm{He})]$ at the same angles is again recorded. Providing that the measurement is performed under identical experimental conditions for both gases, and the flow in the capillary array is collisionless then either of the following two relations[15] may be used to obtain the ratio of cross sections:

$$\sigma_\theta(\mathrm{Ar,Kr})/\sigma_\theta(\mathrm{He}) = [\dot{N}_e(\mathrm{Ar,Kr})/\dot{N}_e(\mathrm{He})]\,[m(\mathrm{He})/m(\mathrm{Ar,Kr})]^{1/2}\,[\dot{N}_b(\mathrm{He})/N_b(\mathrm{Ar,Kr})] \quad (1)$$

$$\cong [\dot{N}_e(\mathrm{Ar,Kr})/\dot{N}_e(\mathrm{He})]\,[p(\mathrm{He})/p(\mathrm{Ar,Kr})]\,, \quad (2)$$

where $\dot{N}_e(\mathrm{Ar,Kr})$ and $\dot{N}_e(\mathrm{He})$ are the count rates of elastically scattered electrons which are detected by the analyzer at the scattering angle θ, m(He) and m(Ar, Kr) are the atomic weights of the respective gases, N_b(He) and N_b(Ar, Kr) are the flow rates of the gases through the capillary array, and p(He) and p(Ar, Kr) are the pressures of the gases behind the capillary array (chamber F3 of Fig. 1, (Ref. 15). For collisional flow, which represents the conditions of these experiments, Eq. 1 is still correct. However, care must be taken to ensure that the mean free path between collisions in the capillary array is nearly identical for the reference gas (He) and the gas to be measured (Ar or Kr).

By the above method we obtain a ratio of the DCS for Ar or Kr to that of He. The absolute value of σ_θ(Ar) or σ_θ(Kr) is calculated by multiplying this ratio by the absolute values of σ_θ(He), recently reported by Register *et al.*[16]

The following precautions were taken during the measurements in order to avoid some of the possible sources of errors.

(1) The energy of the incident electron beam was calibrated using the 19.36-eV resonance in He, and is known to an accuracy of ±0.05 eV.

(2) The true zero scattering angle was determined from the symmetry of the scattering intensity corresponding to the $2\,^1P$ excitation in He.

(3) The incident electron current was monitored by a Faraday cup. In all our measurements this current was found to be constant within ±3% over the duration of the experiment. The electron gun was differentially pumped. Therefore, changing Ar or Kr to He did not affect the incident current.

(4) The contribution of the background scattering (both the direct electron beam contribution and scattering by the background gas) to the scattering from the target gas beam was measured by providing an alternate leak to the vacuum chamber.

The flow to the chamber was switched from the capillary array to the alternate gas inlet and the proper background pressure for desired gas was established. The angular distribution of the scattered electron intensity was then measured. It was found that above 20° scattering angle the background scattering was between 1% to 2% of the scattering from the beam formed by the capillary array.

The experimentally determined angular distributions have been fitted to a partial wave expansion as described previously by Register *et al.*[16] This procedure yielded an independent check on our normalization procedure at impact energies below the first inelastic threshold and served as a guide in extrapolating the differential cross sections to 0° and to 180°.

III. RESULTS AND DISCUSSION

Using the method described in the preceding section, the ratios, $\sigma_\theta(\mathrm{Ar,Kr})/\sigma_\theta(\mathrm{He})$, were measured at electron impact energies of 3, 5, 7.5, 10, 15, 20, 30, 50, 75, and 100 eV. At each impact energy an angular range of 20° to 135° was covered. These ratios were then multiplied by the recently measured values of helium σ_θ(He) (Ref. 16) and absolute values of σ_θ(Ar) and σ_θ(Kr) were obtained. For the sake of clarity the Ar and Kr results will be discussed separately.

A. Argon differential cross sections

Table I presents the σ_θ(Ar) values as determined by the relative-flow technique [Eq. (1)]. Typical angular distributions at 3, 20 and 100 eV impact energies are shown in Figs. 1, 2, and 3. At all impact energies studied in the present experiments two minima are found between 20° and 135°. Measurements were made every 5° except in regions of deep minima where the data were collected every 1° until the minima were found. Table II summarizes the positions of these minima at each electron-impact energy. The angular resolution of our spectrometer is ±2°. The positions of these minima are uncertain to ±2°.

We have chosen the 3, 20, and 100 eV data as representative for comparing our results with others. This choice was influenced by the fact that at these energies cross sections are available for comparison.

At 3-eV (Fig. 1) electron-impact energy the present results are compared with the measurements of Andrick,[7] Ramsauer and Kollath,[17] and the theoretical calculations of Walker[18] (which take into consideration exchange and a polarization po-

TABLE I. Elastic differential cross sections σ_θ(Ar) at electron-impact energies E_0 and scattering angles θ in units of 10^{-21} m^2/sr. Quantities shown in parentheses have been obtained by extrapolation. The estimated error in the values of σ_θ(Ar) is 20%.

θ (deg) \ E_0 (eV)	3	5	7.5	10	15	20	30	50	75	100
20	1.7	6.3	22	51	93	70	50	38	24	18
25	2.2	4.6	17	39	76	53	41	28	16	10
30	3.1	5.0	14	30	60	41	32	19	10	6.0
35	4.1	5.9	12	23	45	30	24	14	6.0	3.6
40	5.1	6.9	12	18	34	24	17	8.6	3.2	2.2
45	6.1	8.4	12	15	26	16	12	5.4	2.0	1.2
50	7.0	10	13	13	15	11	7.8	3.2	1.1	0.72
55	7.3	11	13	11	9.0	6.1	4.0	1.4	0.40	0.51
60	8.9	11	14	11	5.4	2.9	1.3	0.31	0.24	0.45
65	8.5	13	14	11	4.2	1.7	0.40	0.028	0.31	0.51
70	8.5	13	13	12	3.4	0.67	0.032	0.24	0.46	0.70
75	8.2	13	14	11	3.4	0.64	0.50	0.86	0.74	1.0
80	7.9	13	13	10	5.2	1.5	1.4	1.5	1.1	1.2
85	7.0	11	11	8.8	6.0	2.4	2.5	2.4	1.5	1.3
90	6.2	8.2	8.6	7.8	6.2	3.8	3.5	3.0	1.8	1.2
95	5.1	6.4	7.2	5.9	5.6	4.7	4.3	3.3	1.9	1.1
100	4.1	4.3	4.5	4.0	4.8	4.8	4.7	3.3	1.9	0.92
105	3.3	2.7	2.9	1.9	4.0	4.6	4.5	3.2	1.5	0.72
110	2.4	1.5	1.1	0.54	2.8	4.2	3.9	2.7	1.1	0.50
115	1.6	0.96	0.54	0.070	2.2	3.5	3.2	2.3	0.74	0.24
120	1.1	0.77	0.93	0.89	2.1	2.9	2.4	1.6	0.44	0.11
125	0.79	1.2	0.45	2.9	2.7	2.7	1.9	1.1	0.23	0.050
130	0.73	1.8	5.0	5.2	4.4	2.6	1.3	0.56	0.15	0.16
135	(0.52)	(3.1)	(8.9)	(9.4)	6.5	2.8	0.68	0.26	0.26	(0.42)

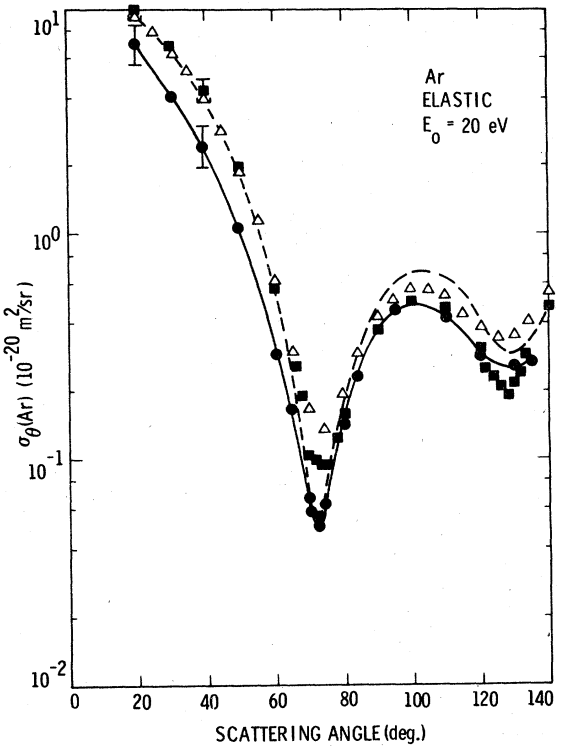

FIG. 2. Elastic differential scattering cross sections for Ar at 20-eV electron-impact energy. ■ Williams and Willis (Ref. 19), △ DuBois and Rudd (Ref. 20), --- Walker (Ref. 18) [exch + pol], ● present, joined by a best visual fit solid line.

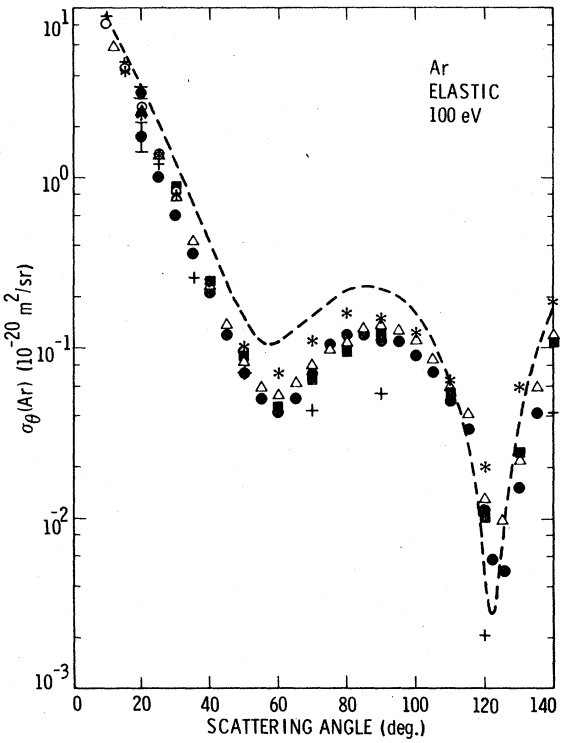

FIG. 3. Elastic differential scattering cross sections for Ar at 100-eV electron-impact energy. ■ Williams and Willis (Ref. 19), △ DuBois and Rudd (Ref. 20), ○ Jansen *et al.* (Ref. 3), * Vuškovič and Krupea (Ref. 21), + Joachain *et al.* (Ref. 23) (Opt. Mod), --- Walker (Ref. 18) (exch + pol), ● present.

tential calculated using the polarized orbital method). The agreement of the present results with the data of Andrick is excellent. Andrick used the phase-shift method to obtain the absolute values of cross sections for the scattering angles from 0° to 180°. Between 30° and 100° the agreement with Ramsauer and Kollath is also satisfactory considering the error limits of the two measurements. However, in other angular regions there are substantial deviations. The predictions of the theory are in good agreement in the region lying between 70° and 140°, but at low angles they are lower than the present results.

Figure 2 compares the present data with the differential cross section values of Williams and Willis[19] and of DuBois and Rudd[20] at 20-eV impact energy. The theoretical predictions of Walker[18] are also shown. It is clear from this figure that our results are considerably lower than the two measurements as well as the theory at low scattering angles. This discrepancy was noted about two years ago. Since then the measurements were repeated several times on two different spectrometers under different experimental conditions. All these measurements agreed to within 20%. Since we use He cross sections for normalization, an error in He cross-section values will affect the present results. These cross-section values have recently been carefully measured in our laboratory[16] and the error in their absolute values have been estimated to be between 5 and 10%. There-

TABLE II. Angles θ_1 and θ_2 corresponding to the first and second minimum, respectively, in Ar and Kr in the angular range between 20° and 135°. The uncertainty in the positions of minima has been estimated to be ±2°.

	Ar		Kr	
E_0 (eV)	θ_1	θ_2	θ_1	θ_2
3	15	135	30	122
5	25	119	35	116
7.5	40	116	55	116
10	60	115		114
15	70	117	75	115
20	73	128	74	130
30	70	135	65	
50	65		52	130
75	60	130	46	104
100	60	124	42	96

fore, a combined error of 21% is obtained for Ar at 20 eV. The error bars for the two measurements are shown in Fig. 2. It is seen that they do not overlap.

At 100 eV several measurements are available. They are compared with the present results in Fig. 3. At low scattering angles our results are found to be lower than other measurements.[3,19-22] The results of Gupta and Rees[22] are not shown but agree very closely with the data of Du Bois and Rudd.[20] The shape of the DCS curve of Vuskovic and Kurepa[21] is in excellent agreement with the present results but the absolute values are higher by about 30%. Comparison has also been made with two recent theoretical calculations. Results of the optical-model calculations of Joachain *et al.*[23] are shown for various scattering angles. Except for high-angle scattering the results of this theory are quite close to the values of the present measurements. The theoretical calculations of Walker[18] agree with the shape of the present DCS curve but in most part are higher by a factor of about 1.9.

The phase shifts obtained from an analysis of the present angular distribution for Ar are summarized and compared with those of Williams[6] and Andrick[7] in Table III. The $L=0$, 1, and 2 phase shifts agree among each other to within about 10% in general, although in some cases deviations of about 20% occur. The uncertainty in the $L=3$ phase shifts are larger but they do not appreciably contribute to the cross sections and are reasonably well given by the Born model. In the present work, the higher partial-wave contributions have been approximated by Born phase shifts. The DCS's calculated from the phase shifts of Table III are in agreement with each other to about 15% and with the DCS's obtained from the He relative-flow normalization. Larger deviations are present at 3 and 20 eV. At 3 eV experimental difficulties and the nature of the DCS curve (not so well pronounced structures) can give rise to much larger uncertainties in the phase-shift fitting. At 20 eV the single electron excitation and ionization channels are open and the normalization of the data on the basis of real phase-shift analysis is no longer applicable. Thus relative-flow normalization is considered more accurate at these energies. This question will be further discussed in connection with the integral cross sections.

TABLE III. Summary of phase shifts for elastic scattering by argon. Numbers in parentheses are interpolated values.

	Phase shift (radian)												
	$L=0$			$L=1$			$L=2$			$L=3$			
E_0 (eV)	Present	Ref. 6	Ref. 7	Present	Ref. 6	Ref. 7	Present	Ref. 6	Ref. 7	Present	Ref. 6	Ref. 7	Born
3	−0.548	−0.457	−0.493	−0.140	−0.134	−0.142	0.125	0.142	0.120	0.035	0.021	0.025	0.024
5	−0.747	(−0.685)	−0.733	−0.256	(−0.205)	−0.277	0.254	(0.317)	0.260	0.102	0.031	0.044	0.041
7.5	−1.051	(−0.919)	(−0.958)	−0.398	(−0.405)	(−0.429)	0.491	(0.620)	0.535	0.125	0.066	0.071	0.061
10	−1.243	−1.098	−1.143	−0.430	−0.528	−0.562	0.805	0.936	0.840	0.171	0.093	0.100	0.081
15	−1.365	−1.394	−1.443	−0.506	−0.750	−0.782	1.593	1.451	1.390	0.200	0.154	0.145	0.122
20	−1.818	−1.653	−1.683	−0.871	−0.935	−0.962	1.679	1.747	1.670	0.262	0.241	0.232	0.162

B. Krypton differential cross section

Differential cross sections for krypton are presented in Table IV. As in the case of Ar, the measurements were made at 5° intervals but near the deep minima of the angular distribution curves

TABLE IV. Elastic differential cross sections, σ_θ(Kr) at electron-impact energies, E_0, and at scattering angles, θ in units of 10^{-21} m^2/sr. Quantities shown in parentheses have been obtained by extrapolation. The estimated error in the measured values of $\sigma(\theta)$ is 20%.

θ (deg) \ E_0 (eV)	3	5	7.5	10	15	20	30	50	75	100
20	8.1	18	50	71	116	93	76	64	35	26
25	6.3	14	39	58	98	86	52	39	20	13
30	5.7	12	31	46	76	57	36	22	9.2	4.8
35	5.9	12	25	38	57	48	25	11	3.6	1.5
40	6.9	12	21	31	44	27	14	4.6	0.97	0.46
45	8.0	13	18	23	30	18	7.7	1.7	0.26	0.42
50	11	14	16	18	21	12	3.8	0.52	0.63	0.96
55	14	16	16	15	13	6.9	1.9	0.54	1.3	1.5
60	15	17	16	13	7.9	4.1	0.99	1.5	1.9	1.9
65	16	18	17	12	5.3	2.6	0.72	1.9	2.4	2.1
70	16	18	17	11	4.4	1.9	1.0	2.2	2.5	1.8
75	15	18	18	11	3.9	1.7	1.4	2.4	2.2	1.5
80	13	17	17	11	4.0	2.1	1.7	2.2	1.6	1.0
85	12	16	15	10	4.4	2.6	2.0	2.0	1.0	0.52
90	9.4	14	12	8.4	4.4	3.0	2.2	1.6	0.57	0.23
95	7.4	10	9.1	6.8	4.3	3.4	2.3	1.3	0.30	0.10
100	5.0	6.4	6.0	4.6	4.4	3.5	2.2	0.95	0.14	0.19
105	3.7	3.9	3.2	2.8	3.6	3.5	2.2	0.64	0.084	0.34
110	1.7	1.8	0.74	1.0	3.4	3.3	1.8	0.40	0.15	0.51
115	0.92	0.49	0.16	0.84	2.8	3.1	1.6	0.27	0.21	0.66
120	0.56	0.69	1.3	1.5	3.2	2.9	1.2	0.17	0.26	0.75
125	0.98	2.3	3.8	3.6	3.5	2.7	0.96	0.089	0.31	0.66
130	1.5	5.0	8.9	7.0	4.9	2.7	0.74	0.062	0.31	0.53
135	(3.0)	(9.0)	(15)	(11)	5.5	(3.3)	(0.63)	0.077	0.27	0.39

data were obtained at 1° intervals. Figures 4, 5, and 6 show the DCS data for 3, 20, and 100 eV electron-impact energies, respectively. Table II presents the angles associated with the minima.

Figure 4 compares the present 3-eV results with the measurements of Heindorff *et al.*[24] Their data are in relative units and have been normalized to the present ones at 70° scattering angle. The results of Ramsauer and Kollath[17] are also presented. It is clear from this figure that the shape of the DCS curve obtained by Heindorff *et al.*[24] agrees very well in the 30° and 100° angular region. The theoretical predictions of Walker[18] are again lower than the present measurements at low scattering angles as has been found in the case of Ar.

In Fig. 5, at 20-eV impact energy, a comparison is made with the experimental results of Williams and Crowe.[25] The present results agree, within error limits, with the measurements of Williams and Crowe at 20° scattering angle. However, at other angles our results are lower. This disagreement is similar to that found in the case of Ar (Sec. III A) and, as mentioned earlier, was discovered about two years ago. Since then we have performed the experiment several times on two different spectrometers under different experimental conditions. The resulting data were

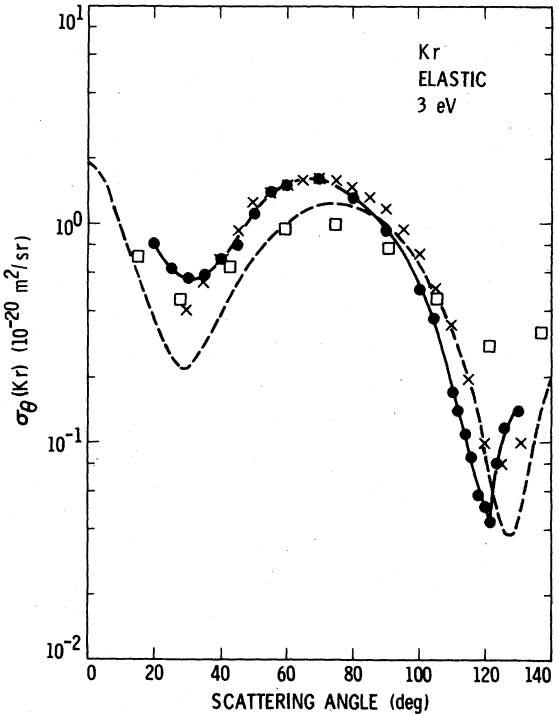

FIG. 4. Differential cross sections for the elastic scattering of 3-eV electrons by Kr. ×Heindörff *et al.* (Ref. 24) (normalized to present results at 70° scattering angle), □ Ramsauer and Kollath (Ref. 17), --- Walker (Ref. 18) (exch+pol), ● present, joined by a best visual fit solid line.

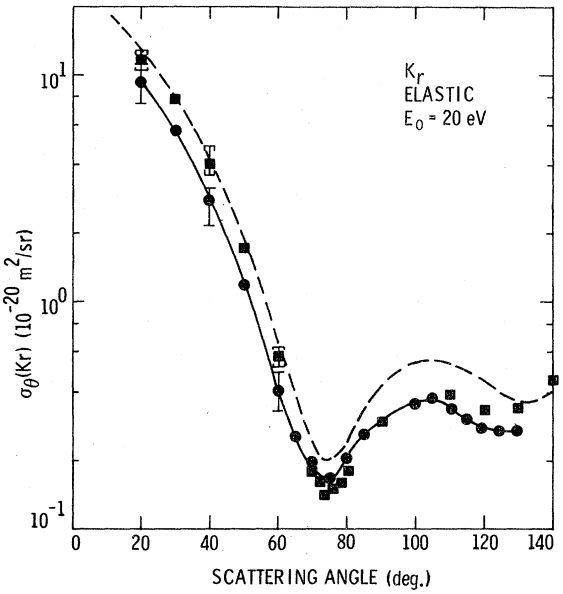

FIG. 5. Elastic differential scattering cross sections for Kr at 20-eV electron-impact energy. ■ Williams and Crowe (Ref. 25), --- Walker (Ref. 18) (exch+pol), ● present, joined with a best visual fit solid line.

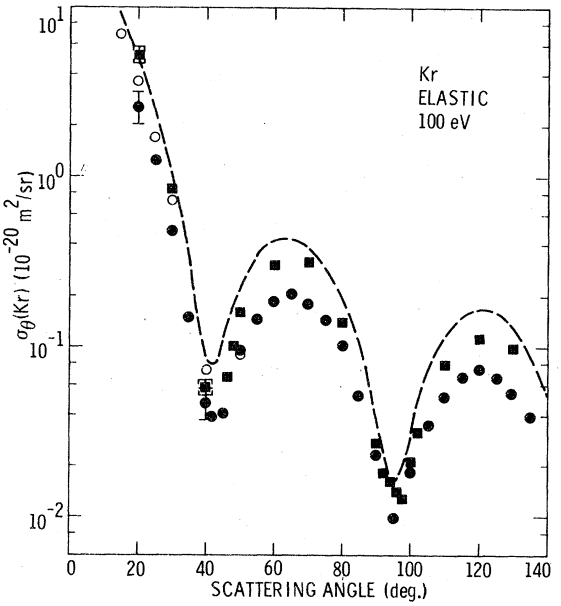

FIG. 6. Elastic differential scattering cross sections for Kr at 100-eV electron-impact energy. ■ Williams and Crowe (Ref. 25), ○ Jansen and de Heer (Ref. 4), --- Walker (Ref. 18) (exch+pol), ● present.

consistent and agreed with each other within 20% which is the error limit of the present measurements. Therefore, the discrepancy between our results and those of Williams and Crowe are difficult to explain at the present time. In Fig. 5 our results at 20 eV are also compared with the recent improved calculations of Walker.[18] It is found that the shape of the present DCS curve agrees with the predictions of the theory but the theoretical values are higher by a factor of about 1.7.

At 100-eV electron-impact energy the situation is similar to that found in the case of Ar. Our results, shown in Fig. 6, are lower than the measurements of Williams and Crowe[25] and Jansen and de Heer.[4] The predictions of Walker's theory are also shown. Once again the shape of the theoretical DCS curve agrees very well with the present results but the absolute values are higher by about a factor of 2.

A phase-shift analysis for Kr was also carried out and the results are given in Table V where they are compared with the phase shifts given in Ref. 24. The validity of analyzing heavy atom scattering data in the frame of the *LS* coupling scheme is questionable. However, it was found that the phase shift normalization and the He relative-flow normalization below 15 eV agreed within about 15% except at the lowest energy (3 eV). At this energy, small changes in the relative shape of the DCS produce large variations in the resulting normalization. The phase shifts which produced the best fit to the shape of 3 eV data gave a normalization approximately 60% larger than that obtained by the relative-flow technique. This difference in normalization is primarily due to the uncertainty in the location of the second minimum

TABLE V. Summary of phase shifts for krypton. (Numbers in parentheses are interpolated values.)

	$L=0$		$L=1$		$L=2$		$L=3$	
E_0 (eV)	Present	Ref. 24	Present	Ref. 24	Present	Ref. 24	Present	Ref. 24
3	−0.692	−0.527	−0.262	−0.195	0.288	0.229	0.093	0.008
5	−0.832	−0.832	−0.352	0.387	0.424	0.510	0.129	0.043
7.5	−1.107		−0.393		0.741		0.176	
10	−1.369	(−1.332)	−0.644	(−0.746)	1.003	(0.995)	0.245	(0.146)
15	−1.586		−0.847		1.329		0.225	

in the DCS. The relative-flow measurements which are not sensitive to this feature are therefore more reliable.

Above 15 eV, excitation and ionization processes make the phase-shift normalization unreliable. However, this technique is convenient for extrapolating the relative DCS to experimentally inaccessible angles (0° to 20° and 135° to 180°) and was used for that purpose in this work.

C. Integral and momentum-transfer cross sections

If the differential cross sections from 0° to 180° are known, then the elastic integral $Q_{\text{elas}}(\text{Ar},\text{Kr})$ and momentum transfer $Q_M(\text{Ar},\text{Kr})$ cross sections can be calculated from the following relations:

$$Q_{\text{elas}} = 2\pi \int_0^{\pi} \sigma_\theta(\text{Ar},\text{Kr}) \sin\theta \, d\theta \,, \tag{3}$$

$$Q_M = 2\pi \int_0^{\pi} \sigma_\theta(\text{Ar},\text{Kr}) \sin\theta (1-\cos\theta) d\theta \,. \tag{4}$$

In the present experiment the measurements were made in the angular range of 20° to 135°. Therefore, cross sections in the region between 0° to 20° and 135° to 180° were needed. The low-angle data (between 0° and 20°) could be obtained from theoretical calculations. However, the present results show that the agreement with the available theoretical data is not very satisfactory. At impact energies which are lower than the first inelastic threshold, one can use the phase-shift analysis method[16] to calculate the values of the cross sections. However, at impact energies above the threshold this same procedure, in principle, is not applicable. In the case of elastic cross sections for He, it was found[16] that the phase-shift method utilizing real phase shifts at high impact energies provided accurate shape of the angular distribution but the absolute values had to be obtained through some normalization procedure. Therefore, for the present extrapolations, the real phase-shift method was used to fit the shape of the Ar and Kr DCS curves in the 20° to 135° region. The normalization factor resulting from this fitting gave reasonable agreement with the cross-section values obtained by the relative-flow technique (present data) at energies lower than the first inelastic threshold. At higher impact energies, the fit to the shape of the 20° to 135° DCS was quite reasonable but the normalization differed significantly. Thus, at all energies the technique adopted for the present measurements was to fit the shape of DCS via a real phase-shift expansion while retaining the normalization from the relative-flow measurements. Details of this method are presented in Ref. 16.

By following the above procedure, cross-section data in the angular regions 0° to 20° and 130° to 180° were obtained. Using Eqs. (3) and (4), integral and momentum-transfer cross sections were then calculated. They are presented and compared with other available data and with cross sections obtained by the phase-shift normalization in Tables VI and VII.

D. Total cross sections

Total scattering cross sections are the sum of cross sections for elastic and all inelastic processes and can be represented by the following relationship:

$$Q_T = Q_{\text{ion}} + Q_{\text{elas}} + Q_{\text{exc}} \,, \tag{5}$$

TABLE VI. Integral and momentum-transfer cross sections for Ar (in 10^{-20} m^2 units). The numbers in parentheses are interpolations.

	Q (from phase shifts)			Q (from He normalization)	Q^M (from phase shifts)				Q^M (from He normalization)
E_0 (eV)	Present	Ref. 6	Ref. 7	Present[a]	Present	Ref. 6	Ref. 7	Ref. 2	Present[a]
3	6.67	5.64	5.74	5.5	5.14	4.68	4.50	4.07	4.1
5	10.03	10.10	9.72	8.4	7.62	9.08	8.26	7.20	6.4
7.5	15.56		(13.5)	13.0	12.76		(14.2)	11.0	11.0
10	20.11	23.34	21.63	18.0	16.61	18.93	17.46	13.8	15.0
15	22.28	23.93	23.92	21.0	16.14	14.33	14.36	13.2	15.0
20	19.74	19.77	19.92	12.5	10.36	9.42	9.74	10.4	6.6
30				9.2				7.2	3.7
50				6.1					2.4
75				4.0					1.9
100				2.6					1.6

[a] The values obtained from the He normalization are considered more reliable than the ones obtained by our phase-shift fitting. Therefore, these values have been used in the present work for various experimental and theoretical comparisons.

TABLE VII. Integral and momentum-transfer cross sections for krypton (in 10^{-20} m^2 units).

	Q		Q^M		
E_0 (eV)	From phase shift	From He normalization [a]	From phase shift	From He normalization [a]	Ref. 2
3	17.18	10.0	13.68	8.0	4.8
5	17.98	14.4	14.28	11.9	10.72
7.5	23.96	18.5	19.17	13.4	15.9
10	27.21	19.4	20.72	11.5	19.4
15	25.05	22.1	13.68	9.7	
20		16.2		4.7	18.0
30		10.4		2.2	
50		8.9		1.3	
75		5.2		0.97	
100		4.0		0.88	

[a] Same as the footnote in Table VI.

where Q_T is the total cross section, Q_{ion} the integral ionization cross section, Q_{elas} the integral elastic cross section, and Q_{exc} the integral cross section for excitation to all bound states.

In Figs. 7 and 8 we have summarized the cross sections occuring in Eq. (5) for Ar and Kr, respectively. The total scattering cross sections above 20 eV were obtained by de Heer *et al.*[5] for Ar and by de Heer *et al.*[5] and Wagenaar[26] for Kr. Total cross sections at low energies were compiled by Kieffer[27] and Massey and Burhop[28] for Ar and Kr, respectively. These data are compared in the figures with the values obtained by us. Both for Ar and Kr, the major contribution to the total scattering cross section comes from elastic scattering but ionization contribution becomes also significant above about 20 eV. In general, our values are somewhat lower than those of the Amsterdam group[5,23] but the results are in agreement within the limits of the combined error bars. At low impact energies the present total scattering cross sections are in good agreement with the values obtained from the summary of data for Ar and Kr by Kieffer[27] and by Massey and Burhop.[28] In Fig. 7 the total scattering cross sections measured by Kennerly and Bonham[29] utilizing time of flight technique is also shown and is in good agreement with our values.

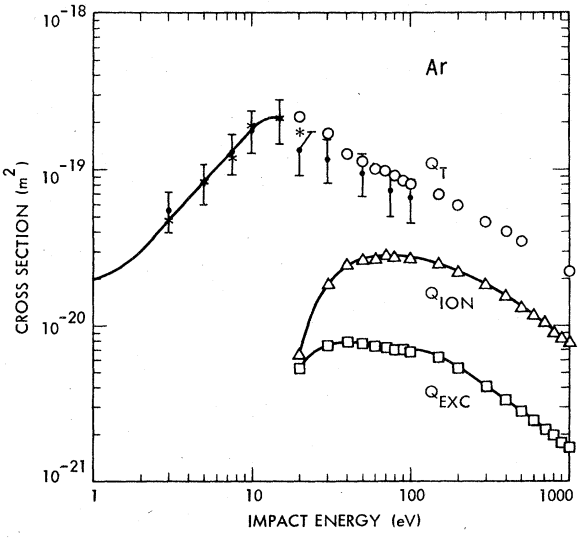

FIG. 7. Total cross sections for Ar. Total scattering cross section: –Ref. 27, ○ Ref. 5, *Ref. 29, ● present values; total ionization cross section, Ref. 5; total excitation cross section, Ref. 5.

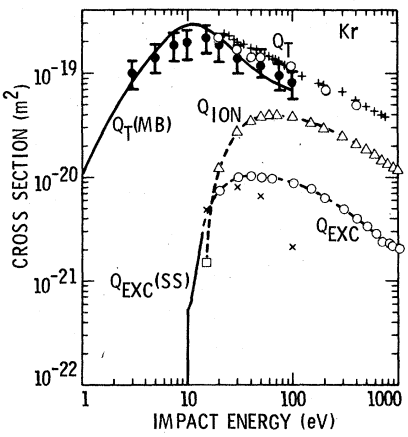

FIG. 8. Total cross sections for Kr. Total scattering cross section: –Ref. 28, +Ref. 26, ○ Ref. 5; total ionization cross section: □ Ref. 30, -△-Ref. 5; Total excitation cross section: –Ref. 31, -○-Ref. 5, ×Ref. 12 (obtained by summing over the lowest 22 electronic states).

TABLE VIII. Various sources of error that contribute to the total error in the measurement of ratio $\sigma(\mathrm{Ar,Kr})/\sigma(\mathrm{He})$.

1. (a) Error in the ratio of flow rates $[\dot{N}_b(\mathrm{He})/\dot{N}_b(\mathrm{Ar,Kr})]$ (Eq. 1)	5%
or	
(b) Error in the ratio of measured pressures $p(\mathrm{He})/p(\mathrm{Ar,\ Kr})$ (Eq. 2).	5%
2. Estimated error in the ratio $[\dot{N}_e(\mathrm{Ar,Kr})/\dot{N}_e(\mathrm{He})]$ (Eq. 1).	2%
3. Estimated error due to the change in the incident electron beam current.	3%
4. Estimated error due to ±2° uncertainty in the relative Ar, Kr DCS.[a]	15%
Total (Square root of the sum of squares)	17%

[a] This error is a combined error which results from the uncertainty in the measurement of angle in the Ar or Kr DCS, the effective path length correction, and the effects of direct beam and background scattering.

E. Error estimation

The ratio, $\sigma(\mathrm{Ar,Kr})/\sigma(\mathrm{He})$, is dependent on several quantities mentioned in Eqs. (1) and (2) and on the scattering angle. Errors in the measurement of these quantities contribute to the total error in the ratio. Table VIII summarizes the various errors. The major error comes from the uncertainty in the measurement of scattering angle, θ. It is seen that the estimated error is about 15%. The value of this error increases for those angular regions where the DCS varies rapidly with the scattering angle as is the case with low-angle data and the data near minima. It is estimated that the overall error in the measurement of the ratio, $\sigma(\mathrm{Ar,Kr})/\sigma(\mathrm{He})$, is about 17%. This estimate is very well supported by several measurements of the value of $\sigma(\mathrm{Ar,Kr})/\sigma(\mathrm{He})$ which were found to lie within 20%. The value of $\sigma(\mathrm{Ar,Kr})$ was then obtained by multiplying the ratio, $\sigma(\mathrm{Ar,Kr})/\sigma(\mathrm{He})$, by the previously measured[16] value of $\sigma(\mathrm{He})$. The estimated error in the value of $\sigma(\mathrm{He})$ is between 5% and 10%. Therefore, the estimated error in the value of $\sigma(\mathrm{Ar,Kr})$ is about 20% which is the square root of the sum of squares in the error of $\sigma(\mathrm{Ar,Kr})/\sigma(\mathrm{He})$ and $\sigma(\mathrm{He})$.

The errors in the integral, Q, and momentum-transfer, Q^M, cross sections are difficult to estimate. It is mainly due to the fact that actual measurements are made in the angular region between 20° and 135°. In the angular regions between 0° and 20° and between 135° and 180° extrapolations are made. For those electron-impact energies which are below the first excitation threshold, phase-shift analysis provides fairly accurate extrapolations. Therefore, the errors in the Q and Q^M are about the same as estimated for $\sigma(\mathrm{Ar,Kr})$, i.e., 20% for the low electron-impact energies. At electron-impact energies above the inelastic threshold the phase-shift analysis is not valid, however, we assume[16] that relative values of differential cross sections are provided by the phase-shift analysis, but the absolute values are not. In the present work, these relative values have been used for extrapolations. The detailed reasoning about these extrapolations can be found in Sec. III C. We estimate that the total errors in the values of Q and Q^M for electron impact energies larger than 15 eV are 30% which comes from the 20% uncertainty in the DCS and about an additional 20% error due to extrapolation.

ACKNOWLEDGMENT

The financial support for this work by the National Aeronautics and Space Administration, Contract No. NAS7-100, and by the Department of Energy, Order No. LS-76-5, is gratefully acknowledged. We are also thankful to Dr. D. Register for the phase-shift analysis of the differential cross sections and for many helpful discussions during the progress of this work. One of us (H.T.) is grateful to NRC-NASA for financial support.

*Permanent address: Department of Physics, Sophia University, Tokyo, Japan.

[1] B. H. Bransden and M. R. C. McDowell, Phys. Rep. 46, 249 (1978).

[2] L. S. Frost and A. V. Phelps, Phys. Rev. 136, A1538 (1964). Numerical values given by L. J. Kieffer, JILA Information Center Report No. 13, University of Colorado, 1973 (unpublished).

[3] R. H. J. Jansen, F. J. deHeer, H. J. Luyken, B. van Wingerden, and H. J. Blaauw, J. Phys. B 9, 185 (1976).

[4] R. H. J. Jansen and F. J. de Heer, J. Phys. B 9, 213 (1976).

[5]F. J. de Heer, R. H. J. Jansen, and W. van der Kaay, J. Phys. B 12, 979 (1979).
[6]J. F. Williams, J. Phys. B 12, 265 (1979).
[7]D. Andrick (private communication, 1973).
[8]Yu. K. Guskov, R. V. Sarrov, and V. A. Slobodyanyuk, Zh. Tekh. Fiz. 48, 277 (1978) [Sov. Phys.—Tech. Phys. 23, 167 (1978)].
[9]A. W. Yau, D. P. McEachran, and A. D. Stauffer, J. Phys. B 13, 377 (1980).
[10]S. P. Khare and A. Kumar, Jr., Pramana 10, 63 (1978).
[11]A. C. Roy and N. C. Sil, J. Phys. B 11, 2729 (1978).
[12]A. Chutjian and D. C. Cartwright, Phys. Rev. A 23, 2178 (1981).
[13]S. Trajmar, S. K. Srivastava, H. Tanaka, and H. Nishimura, and D. C. Cartwright, Phys. Rev. A 23, 2167 (1981).
[14]A. Chutjian, J. Chem. Phys. 61, 4279 (1974); Rev. Sci. Instrum. 50, 347 (1979).
[15]S. K. Srivastava, A. Chutjian, and S. Trajmar, J. Chem. Phys. 63, 2659 (1975).
[16]D. F. Register, S. Trajmar, and S. K. Srivastava, Phys. Rev. A 21, 1134 (1980).
[17]C. Ramsauer and R. Kollath, Ann. Phys. Leipzig 5, 837 (1932).
[18]D. W. Walker (private communication, 1978), J. Phys. B 3, 788 (1970).
[19]J. F. Williams and B. A. Willis, J. Phys. B 8, 1670 (1975).
[20]R. D. DuBois and M. E. Rudd, J. Phys. B 9, 2657 (1976).
[21]L. Vuškovič and M. V. Kurepa, J. Phys. B 9, 837 (1976).
[22]S. C. Gupta and J. A. Rees, J. Phys. B 8, 1267 (1975).
[23]C. J. Joachain, R. Vanderpoorten, K. H. Winters, and F. W. Byron, J. Phys. B 10, 227 (1977).
[24]T. Heindörff, J. Hofft, and P. Dabkiewicz, J. Phys. B 9, 89 (1976).
[25]J. F. Williams and A. Crowe, J. Phys. B 8, 2233 (1975).
[26]R. W. Wagenaar, FOM Report No. 43.948, Amsterdam, Holland (1978); R. J. Wagenaar and F. J. de Heer, J. Phys. B 13, 3855 (1980).
[27]L. J. Keiffer, At. Data 2, 293 (1971).
[28]H. S. W. Massey, E. H. S. Burhop, and H. B. Gilbody, *Electronic and Ionic Impact Phenomena* (Oxford University Press, Oxford, 1969), Vol. I, p. 25.
[29]R. A. Bonham and R. E. Kennerly (private communication, 1979).
[30]D. Rapp and P. Englander-Golden, J. Chem. Phys. 43, 1464 (1965).
[31]M. Schaper and H. Scheibner, Beitr. Plasmaphys. 9, 45 (1969).